

1 **Title**

2 **An improved method for the GC-MS determination of polycyclic aromatic**
3 **hydrocarbons and *n*-alkanes in speleothems**

4

5 **Authors**

6 Elena Argiriadis^{1*}, Rhawn D. Denniston², Carlo Barbante^{1,3}

7

8 **Affiliation**

9 ¹Ca' Foscari University of Venice, Department of Environmental Sciences, Informatics and Statistics, Via Torino 155,
10 30172 Venice, Italy

11 ²Cornell College, Department of Geology, 600 First Street SW Mount Vernon, IA 52314-1098, USA

12 ³Institute for the Dynamics of Environmental Processes CNR-IDPA, Via Torino 155, 30172 Venice, Italy

13

14

15 *Corresponding author, email: elena.argi@unive.it, telephone: +39 041 234 8658, ORCID iD: 0000-
16 0001-7227-405X

17

18 **Abstract**

19 The interest in paleoenvironmental reconstructions from biomarkers in speleothems is increasing,
20 thanks in part to the capacity of speleothems to grow continuously and to resist post-depositional
21 alteration. In particular, the possibility exists to link high-resolution and accurately dated fire and
22 vegetation records with isotopic data of climatic and paleoenvironmental interactions at the local
23 and regional scale. However, the scarcity of existing methods for the quantification of organic
24 molecules in stalagmites, together with the issues of sample availability, contamination, and low
25 concentrations, complicate this approach. In this work, we developed a novel method for the
26 simultaneous determination of 18 polycyclic aromatic hydrocarbons (PAHs) and 26 *n*-alkanes (C₁₀-
27 C₃₅) and then tested it on “clean” calcite and aragonite stalagmite samples from cave KNI-51 in the
28 Australian tropics. The method involves subsampling by using a handheld drill, then the complete
29 dissolution of the matrix in hydrochloric acid, followed by liquid-liquid extraction and GC-MS
30 analysis. Sample preparation was carried out in a 10,000 class clean room, entirely built in stainless
31 steel, to avoid contamination. Detection limits were 0.3-9 ng for PAHs and 6-44 ng for *n*-alkanes.
32 Measurable concentrations of fire-derived PAH compounds, namely phenanthrene, pyrene,
33 benzo(*e*)pyrene and indeno(123-*cd*)pyrene, were detected only in one sample, which dates to the
34 year ~AD 2004, when a fire burned vegetation over the cave; *n*-alkanes were detected in all samples
35 in the range C₂₃-C₃₅, with no odd-even preference.

36

37 The knowledge and use of biomarkers as proxies for paleoenvironmental change is rapidly
38 expanding in concert with a growing demand for such records. Speleothems are important
39 paleoenvironmental proxies due to their capacity for continuous growth, high temporal resolution,
40 precise and accurate age dating by U/Th methods, and strong post-depositional stability¹. In
41 addition, speleothems record a variety of paleoenvironmental events through numerous chemical,
42 mineralogical, and sedimentological signals^{2,3}. Thus, improving our understanding of biomarkers in
43 speleothems represents an important goal. However, due to the dynamics of the deposition process
44 and the inorganic nature of the matrix, concentrations of organic compounds in speleothems are
45 usually very low, close to method and instrumental detection limits⁴. As a result, high amounts of
46 extractable material are required in order to perform a reliable analysis, which in the case of
47 speleothems can be a substantial challenge. In this context, the sources of contamination from
48 sampling, cutting and laboratory operations must be minimized. The need for high sensitivity, low
49 contamination techniques in speleothems are therefore undeniable. In addition, little work has
50 tested the capacity of karst hydrologic systems to transport organic compounds through the
51 bedrock and into cave dripwater at sufficient temporal scales so as to allow for identification of
52 discrete events, such as fires.

53 We focused our research on developing a method for the simultaneous analysis of two classes of
54 hydrocarbons in speleothems, namely 18 polycyclic aromatic hydrocarbons (PAHs) and 26 *n*-
55 alkanes, with the aim of minimizing external contamination and improving the sensitivity of
56 instrumental determination. The use of PAHs as tracers of past combustion processes is well-
57 established⁵, and their persistence in the environment allows detection in several
58 paleoenvironmental archives, including speleothems^{4,6}. Numerous studies, especially on lake
59 sediments and peat, have demonstrated the relation of *n*-alkanes with vegetation changes and
60 associated climatic conditions⁷⁻¹⁰. Relating fire activity and vegetation composition to temperature
61 and precipitation reconstructions achieved through the oxygen and carbon isotopic ratios of
62 speleothems will allow a more in-depth understanding of the interplay between climate and fire at
63 local and regional scales.

64 To date, protocols for the extraction of organic molecules from speleothems include several steps
65 to prevent contamination and maximize recovery, such as solvent washing and acid digestion¹¹⁻¹³.
66 Although previously published methods for the analysis of lipid biomarkers in speleothems allowed
67 accurate and high-resolution determination and have become quite well-established¹², only one

68 method has involved the quantification of PAHs in stalagmites⁶. Briefly, the latter involved crushing
69 the stalagmite fragments into a powder and extracting them with ultrasounds, before Florisil
70 purification and HPLC-fluorescence analysis. Here, we describe the development of a new analytical
71 method based on the complete dissolution of the matrix, followed by a liquid-liquid extraction and
72 GC-MS determination. All steps aim at minimizing contamination while maximizing the analyte yield
73 and thereby allow for a more routine measurement of target compounds in speleothems.

74

75 **Experimental Section**

76 *Materials*

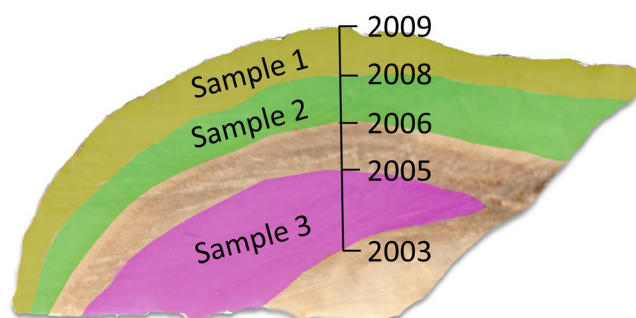
77 Pesticide-grade dichloromethane, *n*-hexane, and acetone and 34-37% SpA hydrochloric acid from
78 Romil Ltd. were employed. Isotope labeled standard solutions (¹³C₆-acenaphthylene, ¹³C₆-
79 phenanthrene, ¹³C₄-benzo(a)pyrene and ¹³C₆-chrysene) were obtained from Cambridge Isotope
80 Laboratories. Native PAHs were acquired from Dr. Ehrenstorfer (PAH Mix-9) and *n*-alkanes (C₁₀-C₃₅
81 solution and hexatriacontane) were acquired from Sigma-Aldrich. All tools and glassware were pre-
82 washed with a 5% Contrad aqueous solution and rinsed three times with *n*-hexane and
83 dichloromethane (DCM), respectively. Where possible, glassware was also muffled at 400 °C.

84

85 *Sampling Methodology*

86 Preliminary tests were run on two types of sample: calcite from Carrara, Italy (granulometry 80-150
87 μm), and portions of an aragonite stalagmite from cave KNI-51, located in the Kimberley region of
88 tropical Western Australia^{14,15}. Three samples (fig. 1) of ~1 g were drilled from the fragment with a
89 handheld Dremel tool at the University of Padua, Department of Geology. Before drilling, the
90 fragment was sonicated three times with *n*-hexane and three times with dichloromethane in order
91 to decontaminate the outer surface. The external layer was removed with the drill and analyzed in
92 order to assess its analyte content. Each tool was cleaned with *n*-hexane and DCM before use and
93 drilling was performed under a fume hood.

94



95

96
97

Figure 1. Subsampling and approximate age relations (in years CE) based on U/Th dating and the zero age of the active growth surface of the stalagmite fragment.

98

99 *PAHs and n-alkanes extraction*

100 Each sample was transferred to a sealed, clean 60 mL vial with a pierceable cap and spiked with a
 101 50 ng of $^{13}\text{C}_6$ -acenaphthylene, $^{13}\text{C}_6$ -phenanthrene, $^{13}\text{C}_4$ -benzo(*a*)pyrene and hexatriacontane as
 102 internal standards before adding 10 mL of DCM. The calcium carbonate matrix was dissolved with
 103 37% Super Purity HCl pre-extracted with dichloromethane to guarantee the absence of organic
 104 contaminants. HCl was added to the samples using a disposable syringe through the vial septum to
 105 avoid evaporation. Samples were kept in an ice bath and mixed by shaking every few minutes until
 106 the reaction was complete, to avoid heating and thus volatilization of lighter analytes⁶. Dissolved
 107 samples were then vortex-extracted three times with 10 mL DCM each. The first aliquot of DCM was
 108 added before the HCl to guarantee the immediate dissolution of the samples in the solvent and
 109 prevent evaporation with the gas developed by the reaction. The extracts were finally collected in
 110 clean glass tubes and evaporated to $\sim 200 \mu\text{L}$ under a gentle stream of nitrogen.

111 In order to test the recovery of the method, several $\sim 0.5 \text{ g}$ aliquots of Carrara calcite were fortified
 112 with known amounts of all native compounds and extracted as described. The method was then
 113 employed for the analysis of stalagmite samples drilled from the fragment shown in fig. 1, together
 114 with several procedural blanks. All operations were run in the class 10,000 cleanroom of Ca' Foscari
 115 University, built entirely in stainless steel and equipped with fume hoods and air filters to guarantee
 116 the lowest external contamination.

117

118

119

120 *GC-MS analysis*

121 PAHs and *n*-alkanes were analyzed with a 7890A GC system coupled to a 5975C single quadrupole
122 mass spectrometer (Agilent Technologies). Compounds were separated through a HP-5ms column
123 (60 m, id 0.25 mm, 0.25 μm film thickness, Agilent Technologies). Operating conditions of the GC
124 for PAHs were as follows: injector temperature 300 °C; transfer line temperature 300 °C; oven
125 temperature program 70 °C for 1.5 min, then 10 °C min^{-1} to 150 °C for 10 min, then 3 °C min^{-1} to
126 300 °C for 15 min, 305 °C for 30 min (postrun); carrier gas (helium) 1 ml min^{-1} ; injection mode,
127 splitless with split valve open after 1.5 min at 50 mL min^{-1} . For *n*-alkanes, the GC program was the
128 following: injector temperature 300 °C; transfer line temperature 300 °C; oven temperature
129 program 50 °C for 5 min, then 18 °C min^{-1} to 315 °C for 16 min, 315 °C for 15 min (postrun); carrier
130 gas (helium) 1.2 ml min^{-1} ; injection mode, splitless with split valve open after 1 min at 50 mL min^{-1} .
131 The mass spectrometer was operated in single ion monitoring mode, using an electron impact
132 source set at 70 eV and 230 °C. The quadrupole temperature was 150 °C. Chromatograms were
133 processed by Agilent MSD Chemstation software. Analytes were quantified by the isotope dilution
134 technique and results for each compound were corrected by the instrumental response factors,
135 obtained by repeated injections of solutions containing all native compounds and internal standards
136 in equal concentrations.

137

138 *Quality control*

139 Procedural blanks were analyzed together with samples in order to assess possible contamination.
140 All $\text{C}_{10}\text{-C}_{35}$ *n*-Alkanes were detected in the range 1-54 abs ng, while for PAHs only naphthalene,
141 phenanthrene, fluoranthene, pyrene, retene, benzo(e)pyrene, benzo(a)pyrene and
142 benzo(ghi)perylene were detected in the range 0.2-4 abs ng. Blank concentrations resulted
143 generally lower those reported in the literature^{6,16}, which underlines the importance of preventing
144 laboratory contamination through “clean” procedures.

145 The detection limits for PAHs, expressed as three times the standard deviation of the blank, range
146 from 0.3 to 9 ng. For *n*-alkanes, the detection limit range is 6-44 ng. Absolute quantities of analytes
147 in samples were corrected by the mean blank values plus three times the standard deviation.

148 Recovery, precision (in terms of relative standard deviation of replicates) and accuracy (percentage
149 relative error with respect to the spiked amounts) were estimated by spiking Carrara calcite with

150 known amounts of native compounds and internal standards: PAH percent recovery was between
151 90 and 163%, precision ranges 0.2-11% and accuracy was 0.2-8%. For *n*-alkanes, recovery was
152 between 43 and 140%, precision was 0.3-34% and accuracy was 0.1-12%. Overall, analytical
153 performances for PAHs are significantly better than the ones of the method by Perrette et al. (2008),
154 confirming that tests carried out on real matrix and complete dissolution of the sample bring
155 significant improvements to the quantification of analytes. Conversely, a direct comparison with
156 literature methods is not possible for *n*-alkanes, since, to the best of our knowledge, none reports
157 such information.

158

159 **Results and discussion**

160 *Fortified samples*

161 The background concentration of analytes in the Carrara calcite was evaluated through repeated
162 analyses and results for the fortified samples were corrected by the mean background values. No
163 PAHs were detected in non-fortified Carrara calcite, while *n*-alkanes were present in low amounts
164 (0.03-0.8 $\mu\text{g g}^{-1}$).

165 *Stalagmite samples*

166 Samples were drilled from the uppermost section of stalagmite KNI-51-11. This sample was
167 collected while actively growing in June 2009 and has been dated by 16 high-precision U/Th
168 methods (two standard deviation errors averaging ± 1.3 year) from CE 1896, including three dates
169 between CE 1999-2009^{14,17}. An age model based on these dates suggests the sampled intervals
170 correspond approximately to CE 2008, 2006-7, and 2003-4. We aimed to test whether burning of
171 the eucalypt savanna over the cave produced PAHs that were transferred via cave drip water into
172 KNI-51 and then incorporated into the stalagmite carbonate. The study of PAHs in stalagmites by
173 Perrette et al. (2008) was complicated by the great depth of the cave and the thick and PAH-rich soil
174 that overlay it. In contrast, soils on the hillslope over KNI-51 are thin, organic-poor, and sparse;
175 rillenkarrn limestone is exposed over much of the landsurface above the cave. In addition, the
176 limestone is fractured, leading to rapid infiltration with little storage of water in the epikarst. As a
177 consequence, issues of PAH storage and re-mobilization in the soil-karst system that plagued
178 Perrette et al. (2008) are not apparent at this site. Fire activity over the cave was assessed for each
179 year between 2001 and 2008 using monthly satellite maps of burn scars created and archived

180 through the North Australia and Rangelands Fire Information website
 181 (<http://www.firenorth.org.au/nafi3/>). These maps reveal that 2004 was the only one of these years
 182 to experience a fire directly over the cave. PAHs were present in measurable abundances only in
 183 sample 3 (~CE 2004), with fluoranthene, pyrene, benzo(*e*)pyrene and indeno(1,2,3-*cd*)pyrene in the
 184 0.3-2 ng g⁻¹ range. The latter was detected also in sample 1 (~CE 2008) (table 1). Thus, it appears
 185 that PAHs formed during burning of the overlying savanna were transported by infiltrating rainwater
 186 into the underlying cave where they were incorporated into stalagmite carbonate, forming a
 187 chemical marker of the fire. In addition, we hypothesize that the thin soils and sloped hillside over
 188 the cave, coupled with the intense monsoonal rainfall regime of the eastern Kimberley (~850 mm
 189 yr⁻¹, with ~80% falling in the austral summer, DJF)¹⁷, quickly eroded residual PAHs from the land
 190 surface such that dripwater contains high PAH abundances only for a short time (perhaps only ~1 yr
 191 in some cases) after each fire.

192 The presence of indeno(1,2,3-*cd*)pyrene, produced by high-temperature combustion¹⁸, in two out
 193 of the three samples requires further investigation to identify the sources and processes involved.
 194 No indeno(1,2,3-*cd*)pyrene was detected in blanks, nor are the sawing and drilling operations likely
 195 to produce such a heavy compound, as they do not reach the high temperatures required. Indeed,
 196 a possible interpretation could be based on its high molecular weight relative to the other PAHs
 197 considered here, which probably enhances its precipitation together with calcite, thus resulting in
 198 an enrichment of this compound in the stalagmite.

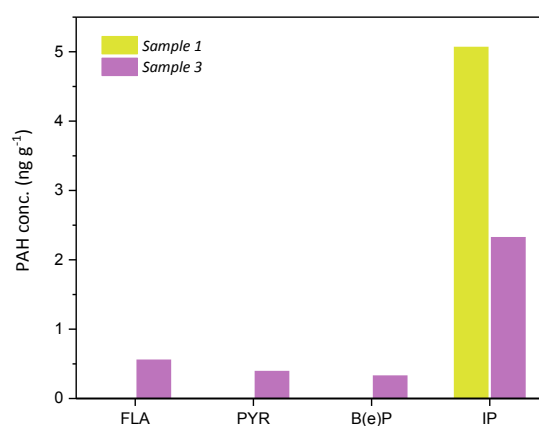
199

200 **Table 1.** PAHs concentrations (ng g⁻¹) in the stalagmite fragment.

	Sample 1 2008	Sample 3 2004	External Layer
Anthracene	nd	nd	4
Fluoranthene	<lod	0.6	nd
Pyrene	<lod	0.4	nd
Benzo(<i>a</i>)anthracene	nd	nd	1
Chrysene	nd	nd	1
Retene	<lod	<lod	nd
Benzo(<i>b</i>)fluoranthene	nd	nd	nd
Benzo(<i>k</i>)fluoranthene	nd	nd	1
Benzo(<i>e</i>)pyrene	<lod	0.3	nd
Benzo(<i>a</i>)pyrene	nd	nd	nd
Benzo(<i>ghi</i>)perylene	nd	nd	<lod
Indeno(1,2,3-<i>cd</i>)pyrene	5	2	nd
Dibenzo(<i>ah</i>)anthracene	nd	nd	nd

201 In Sample 2 (2006-7) all compounds were below the limit of detection, while the external layer
202 contained detectable amounts of anthracene, benzo(a)anthracene, chrysene and
203 benzo(k)fluoranthene between 1 and 4 ng g⁻¹. Such compounds differ completely from the ones
204 detected in samples and blanks, indicating that, if contamination is the source of PAHs in the
205 external layer, it did not affect the inner part and is likely not ascribable to laboratory operations.

206 Cave KNI-51 fills with floodwaters multiple times per decade, and sediments mobilized during these
207 flood events become deposited on stalagmite caps when flood waters recede and then trapped
208 within stalagmites when cave dripwaters resume. As these flood layers can be difficult to avoid
209 when milling stalagmite carbonate, we conducted a test of the impact of these sediments on the
210 PAH abundances measured in KNI-51-11 in case they, rather than the carbonate itself, were the
211 source of the PAHs identified in our analysis. Ten sediment samples from the cave passage were
212 collected from the stalagmite room of KNI-51 and these samples were processed according to the
213 same methods. As expected, given the higher organic content of sediments, PAH abundances in
214 these sediments were higher than those measured in the stalagmite carbonate (Table S1) and thus
215 incorporation of flood detritus within the stalagmite could increase the overall measured PAH
216 concentration. However, no visible flood detritus was present in Samples 1-3 and no insoluble
217 residue was present after digestion in HCl. In addition, PAH compounds detected in the stalagmite
218 samples do not fully coincide with the one present in sediments (Table 1 and S1). For instance, no
219 retene or benzo(a)pyrene were found in calcite. This suggests a differentiation in the deposition
220 dynamics and only a partial influence of sediments on the PAH composition of stalagmites.

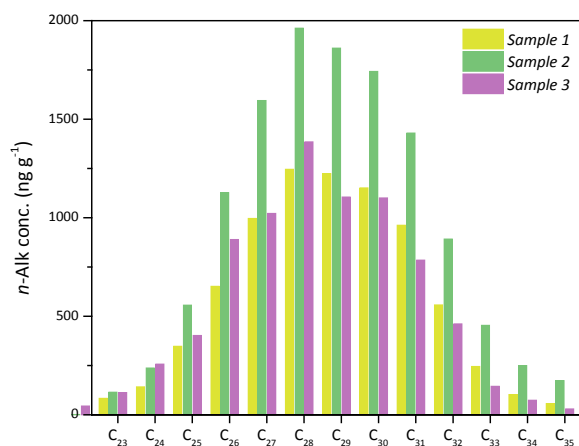


221 **Figure 2.** PAHs concentrations (ng g⁻¹) in samples from the stalagmite fragment.
222

223

224 Only high molecular weight (HMW) *n*-Alkanes in the range C₂₃-C₃₅ were present in all samples and
225 in the external layer and no marked odd-even preference was present⁷. The *n*-alkane distribution is
226 the same in all samples and centered on the C₂₇-C₃₁ interval; sample 2 displayed the highest
227 concentrations (0.1-2 µg g⁻¹). These findings are coherent with literature aliphatic hydrocarbons
228 stalagmite data and likely indicate the presence of another source beside plant residues in soil^{4,19}.
229 Caves are known to host bacterial and fungal communities, which are able to produce and rework
230 lipid compounds²⁰ and are involved in the precipitation of calcium carbonate^{21,22}. As pointed out by
231 Xie et al. (2003), the presence of microbes contributing to the distribution of *n*-alkanes complicates
232 the interpretation of these data. Future assessment of longer time series from KNI-51 stalagmites
233 and the use of specific indexes therein will be required to disentangle the two signals and help in
234 source attribution.

235



236

237

Figure 3. *n*-Alkane concentrations (ng g⁻¹) in samples from the stalagmite fragment.

238

239

240

241

242

243

244

245

246

247

248

249 **Table 2.** *n*-Alkanes concentrations (ng g⁻¹) in the stalagmite fragment.

	Sample 1 2008	Sample 2 2006-7	Sample 3 2004	External Layer
C22	<lod	2	39	20
C23	77	130	97	115
C24	131	269	221	213
C25	320	629	346	429
C26	600	1274	765	752
C27	917	1802	879	1049
C28	1147	2217	1191	1316
C29	1126	2103	950	1276
C30	1059	1969	946	1236
C31	885	1616	675	1061
C32	513	1008	397	644
C33	226	513	124	299
C34	95	282	64	139
C35	52	196	26	89

251

252

253 **Conclusions**

254 We have refined a method for the analysis of organic compounds in aragonite speleothems, based
 255 on complete digestion of the matrix followed by liquid-liquid extraction. This approach minimizes
 256 external contamination and sample amount while increasing analyte recoveries. To our knowledge,
 257 this is the only method for PAH determination in stalagmites besides the one proposed by Perrette
 258 et al. (2008). Quality check showed that, compared to the latter, our protocol has considerably
 259 better analytical performance. The method is also quite easily and quickly applicable on a routine
 260 basis in any chemical laboratory, since it does not require complex instrumentation. In addition, the
 261 wide number of analytes included increases the amount of information obtained from the record
 262 without further sample demand, a significant added value in terms of resolution and considering
 263 the scarce sample availability and the sampling effort required for speleothems.

264 The purpose of this work was to provide a valid tool to the developing field of organic proxy
 265 determination in speleothems. Our method was thus tested on samples from an aragonite
 266 stalagmite from cave KNI-51, which based on the preliminary results, appear to trace documented
 267 fire events. In the future, this technique will be applied to multi-decadal/centennial-scale intervals
 268 to obtain a high-resolution fire reconstruction to be compared with vegetation history and
 269 hydroclimate information provided by isotopic ratios in the same stalagmites.

270 **Acknowledgements**

271 This research was supported by US National Science Foundation EAGER grant DEB-1812476, (PI
272 Rhawn Denniston). The research leading to these results has also received funding from the
273 European Research Council under the European Union's Seventh Framework Programme
274 (FP7/2007–2013)/ERC Grant agreement n° 267696 – EARLYhumanIMPACT. We would like to
275 acknowledge Dr. Patrizia Ferretti (Ca' Foscari University) and Dr. Nereo Preto (University of Padua)
276 for their technical support, John Cugley, David Woods, William Humphreys, Donna Cavlovic, and
277 Steve Stevets for assistance with fieldwork, and Nathan Conner, Jai Lathan, and Ian Radford for
278 introducing the authors to, and providing assistance with, the NAFI program.

279

280 References

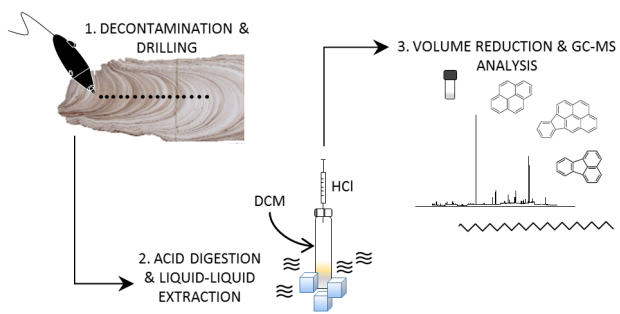
- 281 (1) Blyth, A. J.; Asrat, A.; Baker, A.; Gulliver, P.; Leng, M. J.; Genty, D. A New Approach to Detecting Vegetation and
282 Land-Use Change Using High-Resolution Lipid Biomarker Records in Stalagmites. *Quat. Res.* **2007**, *68* (3), 314–
283 324.
- 284 (2) Fairchild, I. J.; Smith, C. L.; Baker, A.; Fuller, L.; Spötl, C.; Matthey, D.; McDermott, F.; E.I.M.F. Modification and
285 Preservation of Environmental Signals in Speleothems. *Earth-Science Rev.* **2006**, *75* (1–4), 105–153.
- 286 (3) Wong, C. I.; Breecker, D. O. Advancements in the Use of Speleothems as Climate Archives. *Quat. Sci. Rev.*
287 **2015**, *127*, 1–18.
- 288 (4) Blyth, A. J.; Hartland, A.; Baker, A. Organic Proxies in Speleothems - New Developments, Advantages and
289 Limitations. *Quat. Sci. Rev.* **2016**, *149*, 1–17.
- 290 (5) Argiriadis, E.; Battistel, D.; McWethy, D. B.; Vecchiato, M.; Kirchgeorg, T.; Kehrwald, N. M.; Whitlock, C.;
291 Wilmshurst, J. M.; Barbante, C. Lake Sediment Fecal and Biomass Burning Biomarkers Provide Direct Evidence
292 for Prehistoric Human-Lit Fires in New Zealand. *Sci. Rep.* **2018**, *8* (1), 12113.
- 293 (6) Perrette, Y.; Poulencard, J.; Saber, A.-I.; Fanget, B.; Guittonneau, S.; Ghaleb, B.; Garaudee, S. Polycyclic Aromatic
294 Hydrocarbons in Stalagmites: Occurrence and Use for Analyzing Past Environments. *Chem. Geol.* **2008**, *251* (1–
295 4), 67–76.
- 296 (7) Bush, R. T.; McInerney, F. a. Leaf Wax N-Alkane Distributions in and across Modern Plants: Implications for
297 Paleocology and Chemotaxonomy. *Geochim. Cosmochim. Acta* **2013**, *117*, 161–179.
- 298 (8) Freeman, K. H.; Pancost, R. D. Biomarkers for Terrestrial Plants and Climate. In *Treatise on Geochemistry*;
299 Elsevier, 2014; Vol. 12, pp 395–416.
- 300 (9) Nott, C. J.; Xie, S.; Avsejs, L. A.; Maddy, D.; Chambers, F. M.; Evershed, R. P. N-Alkane Distributions in
301 Ombrotrophic Mires as Indicators of Vegetation Change Related to Climatic Variation. *Org. Geochem.* **2000**, *31*
302 (2–3), 231–235.
- 303 (10) Pancost, R. D.; Baas, M.; Van Geel, B.; Sinninghe Damsté, J. S. Biomarkers as Proxies for Plant Inputs to Peats:
304 An Example from a Sub-Boreal Ombrotrophic Bog. *Org. Geochem.* **2002**, *33* (7), 675–690.
- 305 (11) Perrette, Y.; Poulencard, J.; Durand, A.; Quiers, M.; Malet, E.; Fanget, B.; Naffrechoux, E. Atmospheric Sources
306 and Soil Filtering of PAH Content in Karst Seepage Waters. *Org. Geochem.* **2013**, *65*, 37–45.
- 307 (12) Blyth, A. J.; Farrimond, P.; Jones, M. An Optimised Method for the Extraction and Analysis of Lipid Biomarkers
308 from Stalagmites. *Org. Geochem.* **2006**, *37* (8), 882–890.
- 309 (13) Wynn, P. M.; Brocks, J. J. A Framework for the Extraction and Interpretation of Organic Molecules in
310 Speleothem Carbonate. *Rapid Commun. Mass Spectrom.* **2014**, *28* (8), 845–854.
- 311 (14) Denniston, R. F.; Villarini, G.; Gonzales, A. N.; Wyrwoll, K.-H.; Polyak, V. J.; Ummenhofer, C. C.; Lachniet, M. S.;

- 312 Wanamaker, A. D.; Humphreys, W. F.; Woods, D.; et al. Extreme Rainfall Activity in the Australian Tropics
313 Reflects Changes in the El Niño/Southern Oscillation over the Last Two Millennia. *Proc. Natl. Acad. Sci. U. S. A.*
314 **2015**, *112* (15), 4576–4581.
- 315 (15) Denniston, R. F.; Ummenhofer, C. C.; Wanamaker, A. D.; Lachniet, M. S.; Villarini, G.; Asmerom, Y.; Polyak, V.
316 J.; Passaro, K. J.; Cugley, J.; Woods, D.; et al. Expansion and Contraction of the Indo-Pacific Tropical Rain Belt
317 over the Last Three Millennia. *Sci. Rep.* **2016**, *6* (1), 34485.
- 318 (16) Blyth, A. J.; Frisia, S. Molecular Evidence for Bacterial Mediation of Calcite Formation in Cold High-Altitude
319 Caves. *Geomicrobiol. J.* **2008**, *25* (2), 101–111.
- 320 (17) Denniston, R. F.; Wyrwoll, K.-H.; Polyak, V. J.; Brown, J. R.; Asmerom, Y.; Wanamaker, A. D.; LaPointe, Z.;
321 Ellerbroek, R.; Barthelmes, M.; Cleary, D.; et al. A Stalagmite Record of Holocene Indonesian–Australian
322 Summer Monsoon Variability from the Australian Tropics. *Quat. Sci. Rev.* **2013**, *78*, 155–168.
- 323 (18) McGrath, T. E.; Chan, W. G.; Hajaligol, M. R. Low Temperature Mechanism for the Formation of Polycyclic
324 Aromatic Hydrocarbons from the Pyrolysis of Cellulose. *J. Anal. Appl. Pyrolysis* **2003**, *66* (1–2), 51–70.
- 325 (19) Xie, S.; Yi, Y.; Huang, J.; Hu, C.; Cai, Y.; Collins, M.; Baker, A. Lipid Distribution in a Subtropical Southern China
326 Stalagmite as a Record of Soil Ecosystem Response to Paleoclimate Change. *Quat. Res.* **2003**, *60* (3), 340–347.
- 327 (20) Ladygina, N.; Dedyukhina, E. G.; Vainshtein, M. B. A Review on Microbial Synthesis of Hydrocarbons. *Process*
328 *Biochem.* **2006**, *41* (5), 1001–1014.
- 329 (21) Bindschedler, S.; Cailleau, G.; Verrecchia, E. Role of Fungi in the Biomineralization of Calcite. *Minerals* **2016**, *6*
330 (2), 41.
- 331 (22) Sanchez-Moral, S.; Canaveras, J. C.; Laiz, L.; Saiz-Jimenez, C.; Bedoya, J.; Luque, L. Biomediated Precipitation of
332 Calcium Carbonate Metastable Phases in Hypogean Environments: A Short Review. *Geomicrobiol. J.* **2003**, *20*
333 (5), 491–500.

334
335

336 **For Table of Contents Only**

337



338